PCCP

PAPER

View Article Online
View Journal | View Issue

Cite this: *Phys. Chem. Chem. Phys.*, 2024, **26**, 21204

Spin–flip equation-of-motion coupled cluster method with singles, doubles and (full) triples: computational implementation and some pilot applications†

Manisha and Prashant Uday Manohar *

Received 3rd June 2024,
Accepted 10th July 2024

DOI: 10.1039/d4cp02265c

rsc.li/pccp

We present our computational implementation of the spin–flip (SF) equation-of-motion (EOM) coupled-cluster (CC) method with singles, doubles, and (full) triples (SDT) within Q-CHEM. The inclusion of triples not only enhances the quantitative accuracy of the SF-EOM-CCSD method but also provides correct qualitative trends in the energy gaps between strongly degenerate states. To assess the accuracy, we compare our SF-EOM-CCSDT results with full configuration interaction (FCI) and complete-active-space self-consistent field second-order (CASSCF-SO) CI benchmarks to study the adiabatic energy gaps in CH_2 and NH_2^+ diradicals, vertical excitation energies in CH radicals and the bond dissociation of the HF molecule. We have implemented SF-EOM-CCSDT using both the conventional double precision (DP) and the single precision (SP) algorithms. The use of SP does not introduce any significant errors in energies and energy gaps, and, due to low cost (relative to DP), turns out to be a promising approach to widen the applicability of EOM-CCSDT to bigger molecules.

1 Introduction

Near-degeneracy in electronic states of molecules poses a formidable challenge in their electronic structure computation due to the prominence of the static electron correlation[1] in addition to the dynamical one. Balanced and effective inclusion of both these is crucial for accurate computation of energy gaps as they have a pivotal role in studying bonding patterns, spectroscopic parameters, thermochemistry, *etc.* Amongst the available computational methods, the EOM-CC[2–18] methods are robust and methods of choice for electronic structure computation of molecules with strongly interacting electronic states in a simple and straightforward single reference (SR)[6,13,19–21] formalism. Other methods such as multi-reference (MR) CC,[22–30] linear response (LR) CC,[20,31–33] symmetry adapted cluster (SAC) configuration interaction (CI),[34,35] similarity transformed (ST)EOM-CC,[13,36] *etc.* approaches are also known to provide similar (or sometimes, equivalent) results.

In EOM-CC,[5–7] the wavefunctions and energies of the desired target states are obtained by diagonalization of the (similarity transformed) CC Hamiltonian matrix expanded in a suitable configuration space (*e.g.*, singly excited, doubly excited, *etc.* configurations), thereby incorporating the mixing of the strongly-interacting states in an efficient manner, ensuring balanced treatment of the static and dynamic correlation. The so-called EOM-CCSD uses single and double substitution for CC vectors as well as EOM eigen-vectors and has a scaling of $O(N^6)$. The same level of truncation for CC as well as EOM vectors also ensures core-extensivity of the EOM-CCSD wavefunction, although it lacks valence-extensivity.[37] Due to core-extensivity, the excitation energies of a chromophore are unaltered by the addition or removal of the non-chromophoric fragment to the chromophore and this feature is, therefore, also referred to as ''size-intensivity''.

The spin–flip (SF)[38–46] formalism is well discussed in the context of EOM-CC as well as some DFT-based approaches. For excitation energies, two variants in EOM-CC, namely EE for (spin-conserving) electronic excitations[5–7] and SF (for spin-flipping excitations) are well known, and they differ slightly in the way that the target states are formulated relative to the reference state. In EE-EOM-CC, the excited determinants in the configuration space are generated by the action of linear excitation operators (the right eigen-vectors) on the reference configuration in which the spins of the electrons are retained during the excitations. In contrast, in SF-EOM-CC, the excitation operators flip the spin of one and only one electron (from α to β), while the spins of the remaining electron(s) are retained. In the case of EE-EOM-CCSD, the total energies of

Department of Chemistry, Birla Institute of Technology & Science-Pilani, Pilani, Rajasthan 333031, India. E-mail: pumanohar@pilani.bits-pilani.ac.in; Tel: +91 (1596) 25 5682

† Electronic supplementary information (ESI) available. See DOI: https://doi.org/10.1039/d4cp02265c

excited states dominated by singly excited character have an accuracy of 0.2 eV[44] with pronounced tendency for systematic overestimation. The SF-EOM-CCSD errors are even smaller. Moreover, the target–target energy gaps are usually much more accurate compared to the reference–target energy gaps. However, for electronic states with stronger degeneracies, such as dark states of polyenes, or some valence states of polyradicals,[15,47–58] where the doubly excited character predominates, the EOM-CCSD accuracy significantly deteriorates. The increased error in these cases is due to some non-dynamical correlation effects that are missed out at the EOM-CCSD level and can be mitigated to some extent by including the effect of triples. Inclusion of full triples results in the EOM-CCSDT[59] method, which has a scaling of $O(N^8)$. Due to this high cost of EOM-CCSDT, several intermediate approximations[14,60–67] were proposed, which includes both iterative and non-iterative approaches. However, these approaches lack the size-intensivity, particularly for charge-transfer type excitations.[68] Moreover, due to non-uniform correlation corrections for reference and target states, the energy gaps estimated by these approaches are even worse than the EOM-CCSD ones, although the total energies are improved relative to EOM-CCSD.[17] Similar formulations in CC-LR,[69] MRCC,[70] *etc.* have also been reported.

The balanced description of the energy gaps can thus be obtained only by employing full triples resulting in the EOM-CCSDT method with increased computational cost as a price to pay. In this article, we present our computational implementation of SF-EOM-CCSDT within the ccman2 suite[71] of Q-CHEM[72] for single-point energy computations. We have also implemented EE-EOM-CCSDT within Q-CHEM and also acknowledge that the method was (elsewhere) successfully implemented, long back, by Bartlett and co-workers.[73] Recognizing the cost-effectivity of the SP algorithms for CCSD and EOM-CCSD variants illustrated by Krylov and co-workers,[74,75] we have employed both DP as well as SP algorithms for the implementation of SF-EOM-CCSDT as well as EE-EOM-CCSDT. Section 2 presents a brief theory of EOM-CC with a focus on SF-EOM-CCSDT and the programmable expressions for the same are presented in the Appendix. In Section 3 we present some applications of SF-EOM-CCSDT and discuss the results. Finally, we present our conclusions in Section 4.

2 Theory

EOM-CC[6,7,36,51,76] theory is discussed in detail in several articles. Here, we present, a brief and, rather, a less rigorous outline of the method just to get a flavor of the practical aspects. Consider the Hamiltonian eigenstates Ψ_0 & Ψ_f. They obey the time-independent Schrödinger equation and we have

$$\hat{H}|\Psi_0\rangle = E_0|\Psi_0\rangle \quad (1)$$

$$\hat{H}|\Psi_f\rangle = E_f|\Psi_f\rangle \quad (2)$$

where, E_0 and E_f are the exact eigenvalues of the respective states. In the EOM formalism, the Ψ_f & Ψ_0 are related by

$$|\Psi_f\rangle = \hat{R}|\Psi_0\rangle \quad (3)$$

where $\hat{R}$ is the linear operator, which we will define later. In the case of EOM-CCSDT, Ψ_0 is the CCSDT wavefunction defined by

$$|\Psi_0\rangle = e^{\hat{T}}|\Phi_0\rangle \quad (4)$$

where $|\Phi_0\rangle$ is a single Slater determinant wavefunction – usually (but not necessarily) the Hartree–Fock wavefunction. $\hat{T}$ is the sum of the one-, two- and three-body excitation operators.

$$\hat{T} = \hat{T}_1 + \hat{T}_2 + \hat{T}_3 \quad (5)$$

$$\hat{T}_1 = \sum_i^{\text{occ}} \sum_a^{\text{virt}} t_i^a a_a^\dagger a_i$$

$$\hat{T}_2 = \sum_{i<j}^{\text{occ}} \sum_{a<b}^{\text{virt}} t_{ij}^{ab} a_a^\dagger a_b^\dagger a_j a_i$$

$$\hat{T}_3 = \sum_{i<j<k}^{\text{occ}} \sum_{a<b<c}^{\text{virt}} t_{ijk}^{abc} a_a^\dagger a_b^\dagger a_c^\dagger a_k a_j a_i \quad (6)$$

In eqn (6) we have set up the convention that will be continued in the article. From now onwards, the indices, $i, j, k, \ldots$ will be used for labelling the occupied orbitals whereas for the virtual orbitals, the indies, $a, b, c \ldots$ will be used.

Substituting eqn (4) in eqn (1) one can solve and simplify to get

$$\hat{H}|\Psi_0\rangle = \hat{H}e^{\hat{T}}|\Phi_0\rangle = E_0 e^{\hat{T}}|\Phi_0\rangle \quad (7)$$

$$e^{-\hat{T}}\hat{H}e^{\hat{T}}|\Phi_0\rangle = (\hat{H}e^{\hat{T}})_C|\Phi_0\rangle = \bar{H}|\Phi_0\rangle = E_0|\Phi_0\rangle \quad (8)$$

$$E_{CC} = E_0 = \langle\Phi_0|\bar{H}|\Phi_0\rangle \quad (9)$$

$$0 = \langle\Phi^*|\bar{H}|\Phi_0\rangle \quad (10)$$

Substituting Φ^* in eqn (10) by Φ_i^a, Φ_{ij}^{ab}, and Φ_{ijk}^{abc}, respectively, would yield the equations for the amplitudes of $\hat{T}_1$, $\hat{T}_2$ and $\hat{T}_3$.

From eqn (2)–(4), it follows

$$|\Psi_f\rangle = \hat{R}e^{\hat{T}}|\Phi_0\rangle$$

$$\hat{H}|\Psi_f\rangle = \hat{H}\hat{R}e^{\hat{T}}|\Phi_0\rangle = E_f\hat{R}e^{\hat{T}}|\Phi_0\rangle \quad (11)$$

In the context of SF-EOM-CCSDT, the operator R is the sum of one-, two- and three-body spin-flipping (SF) excitation operators.

$$\hat{R}_1^{SF} = \sum_i^{\text{occ}} \sum_a^{\text{virt}} r_i^a a_{a,\beta}^\dagger a_{i,\alpha} \quad (12)$$

$$\hat{R}_2^{SF} = \sum_{i<j}^{\text{occ}} \sum_{a<b}^{\text{virt}} r_{ij}^{ab} a_{a,\beta}^\dagger a_{b,\delta}^\dagger a_{j,\delta} a_{i,\alpha} \quad (13)$$

$$\hat{R}_3^{SF} = \sum_{i<j<k}^{occ} \sum_{a<b<c} r_{ijk}^{abc} a_{a,\beta}^{\dagger} a_{b,\delta}^{\dagger} a_{c,\delta}^{\dagger} a_{k,\delta} a_{j,\delta} a_{i,\alpha} \quad (14)$$

The operators, $\hat{R}_1$, $\hat{R}_2$ and $\hat{R}_3$, respectively, are very similar to the $\hat{T}_1$, $\hat{T}_2$ and $\hat{T}_3$ operators in CC, except that in $\hat{R}$, the excitation(s) is (are) associated with flipping of the spin of one (and only one) of the electrons from α to β (from $m_s = 1/2$ to $m_s = -1/2$). The spins of the remaining electrons are essentially retained ($\delta \rightarrow \delta$, where $\delta = \alpha$ or β). Clearly, $\hat{R}$ and $\hat{T}$ commute and eqn (11) simplifies to

$$\hat{H}|\Psi_f\rangle = \hat{H}\hat{R}e^{\hat{T}}|\Phi_0\rangle = \hat{H}e^{\hat{T}}\hat{R}|\Phi_0\rangle = E_f e^{\hat{T}}\hat{R}|\Phi_0\rangle$$
$$\bar{H}\hat{R}|\Phi_0\rangle = E_f\hat{R}|\Phi_0\rangle \quad (15)$$

Action of $\hat{R}$ on $\bar{H}$ in eqn (8) would give

$$\hat{R}\bar{H}|\Phi_0\rangle = E_{CC}\hat{R}|\Phi_0\rangle \quad (16)$$

Subtracting the RHS of eqn (16) from eqn (15), it follows

$$(\bar{H} - E_{CC})\hat{R}|\Phi_0\rangle = (E_f - E_{CC})\hat{R}|\Phi_0\rangle \quad (17)$$

Eqn (17) can be transformed into matrix eigenvalue equation.

$$\begin{pmatrix} \bar{H}_{SS} - E_{CC} & \bar{H}_{SD} & \bar{H}_{ST} \\ \bar{H}_{DS} & \bar{H}_{DD} - E_{CC} & \bar{H}_{DT} \\ \bar{H}_{TS} & \bar{H}_{TD} & \bar{H}_{TT} - E_{CC} \end{pmatrix} \begin{pmatrix} R_1 \\ R_2 \\ R_3 \end{pmatrix} = \omega \begin{pmatrix} R_1 \\ R_2 \\ R_3 \end{pmatrix} \quad (18)$$

where, the roots, $\omega = E - E_{CC}$, would give the SF excitation energies of the respective target states. It is important to note that the CC Hamiltonian matrix in eqn (18) being non-hermitian, the left and right eigenvectors are not hermitian conjugates but can be chosen to be mutually biorthogonal. The solution of eqn (18) is good enough to obtain the excitation energies and the corresponding right eigenvectors. The left eigenvectors are required only if one aims to compute gradients and/or properties. Complete diagonalization of the CC Hamiltonian matrix eqn (18) is impractical as we are usually interested in computing only a few electronic states. Davidson's iterative diagonalization procedure[77,78] effectively eliminates the requirement for full diagonalization of the CC Hamiltonian and provides a cost-effective, pragmatic tool to compute the required roots of the matrix. The programmable expressions for the same in the SF-EOM-CCSDT context are provided in the Appendix.

3 Results and discussion

3.1 Computational details

All the EOM-CC(SD and SDT) calculations were performed using a development version of Q-CHEM.[79] For the methylene diradical (CH_2) and nitrenium diradical cation NH_2^+, respectively, the FCI/TZ2P and CISD/TZ2(f,d) optimized structures[80,81] were used. The single-point computations presented in this article have also been performed using the same bases (TZ2P for CH_2 and TZ2(f,d) for NH_2^+). For CH radicals, the experimental ground state equilibrium bond length (r(CH) = 1.1198 Å) was taken from Slipchenko *et al.*[82] The single-point computations were done using cc-pVTZ basis. For bond-breaking of HF, the 6-31G basis was used. The bond distances and the FCI and EOM-CCSD results were taken from ref. 41. The SF-EOM-CCSDT computations using both DP and SP algorithms are presented for all the molecules. The core-orbitals are frozen in post-Hartree–Fock calculations only for the CH radical.

3.2 Adiabatic excitation energies of CH_2 and NH_2^+ diradicals

CH_2 and NH_2^+ diradicals are isoelectronic species with strong static electron correlation. Both these molecules have a triplet ground state of $^3B_1$ character. The ground state UHF wavefunction (M_S = +1 of $^3B_1$; electronic configuration: $1a_1^2 2a_1^2 1b_2^2 3a_1 1b_1$) is taken as the reference configuration for the SF-EOM computations. Fig. 1 presents the isodensity surfaces of the frontier molecular orbitals (MOs) of the CH_2 diradical and the schematic diagram showing the relationship between the SF-EOM reference and target states. The frontier orbitals of NH_2^+ are qualitatively the same.

Tables 1 and 2 summarise the adiabatic excitation energies for CH_2, and NH_2^+, respectively.

For the CH_2 diradical, the excitation energies computed by all the methods are overestimated relative to FCI. The SF-EOM-CCSDT computed excitation energies are overestimated by 0.01 eV or less (for both DP and SP), whereas the SF-EOM-CCSD values are overestimated by 0.044 eV or less.

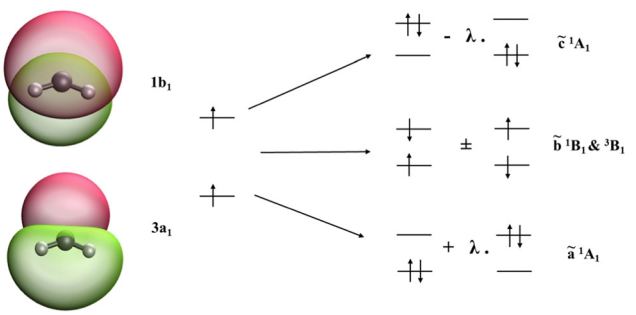

Fig. 1 Frontier MOs of CH_2; the high spin reference configuration and dominant configuration of the SF target states obtained *via* SF-excitations.

Table 1 Total energies of the ground state ($\tilde{X}^3B_1$) and adiabatic excitation energies (eV) of CH_2

Method	$\tilde{a}^1A_1$	$\tilde{b}^1B_1$	$\tilde{c}^1A_1$
FCI[a]	0.483	1.542	2.674
SF-EOM-CCSD	0.517	1.565	2.718
SF-EOM-CCSD(fT)[b]	0.500	1.552	2.688
SF-EOM-CCSD(dT)[b]	0.496	1.548	2.678
SF-EOM-CCSDT	0.493	1.545	2.677
SF-EOM-CCSDT(SP)	0.493	1.545	2.677

[a] From ref. 80. [b] From ref. 68.

Table 2 Adiabatic excitation energies (eV) of NH_2^+ relative to the ground state ($\tilde{X}^3B_1$)

Method	$\tilde{a}^1A_1$	$\tilde{b}^1B_1$	$\tilde{c}^1A_1$
CASSCF SOCI[a]	1.281	1.935	3.380
SF-EOM-CCSD	1.306	1.918	3.420
SF-EOM-CCSD(fT)[b]	1.292	1.905	3.391
SF-EOM-CCSD(dT)[b]	1.289	1.902	3.382
SF-EOM-CCSDT	1.288	1.926	3.386
SF-EOM-CCSDT(SP)	1.288	1.926	3.386
Expt.[c]	1.306 ± 0.010		

[a] From ref. 81. [b] From CCSDT.[68] [c] From ref. 58.

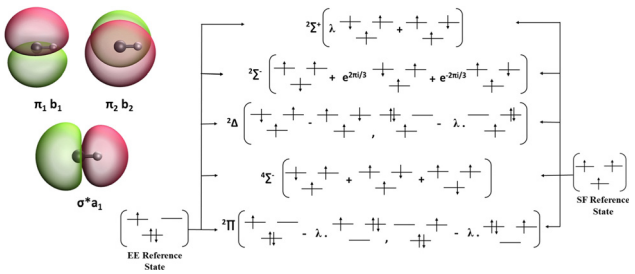

Fig. 2 Frontier MOs in CH and schematic representation of the reference–target relationships in EE-EOM *versus* SF-EOM variants. The target state configurations are spin-conserving excitations relative to the EE reference, whereas the spin-flipping excitations are relative to the SF reference.

The trends in NH_2^+ are more or less the same. Relative to CASSCF-SOCI, the EOM computed excitation energies are systematically overestimated for the two $^1A_1$ states, whereas systematically underestimated for the $^1B_1$ state. The SF-EOM-CCSDT excitation energies differ from the CASSCF-SOCI ones by 0.01 eV or less. The $^1B_1$ state is a typical example where approximate triples fail to provide the qualitatively correct trend. As we go from CCSD to CCSD(fT) and CCSD(dT), the perturbative corrections rather worsen the EOM-CCSD values. However, the use of the rigorous EOM-CCSDT method rectifies the trends with the excitation energy underestimated relative to CASSCF-SOCI by only 0.009 eV, for both DP and SP algorithms.

3.3 Vertical excitation energies of the CH radical

The CH radical has a $^2\Pi$ ground state and is two-fold degenerate with respect to the MO configuration. The vertical excitation energies of this molecule can be computed using two variants, namely, EE and SF. The isodensity surfaces of the frontier MOs, namely, the σ* and the two π orbitals are presented in Fig. 2 along with the schematic diagram showing the relationship between EE/SF reference states and various target states.

For EE, one uses the doublet ground state reference ($\tilde{X}^2\Pi$, M_S = +1/2) and target states are obtained using the EE-EOM-CCSDT approach. For SF, one uses the high-spin quartet reference ($^4\Sigma$, M_S = +3/2) and the target states are obtained as spin-flipped excitations. For both EE-EOM as well as SF-EOM, the energies were computed using both UHF and ROHF references. The total energy of the ground state ($\tilde{X}^2\Pi$) (in Hartrees) and excitation energies of various states (in eV) are summarized in Table 3.

Due to the structural difference between the EE and SF variants, two distinct features are observed in the results. Firstly, due to the non-uniform distribution of the unpaired electron between the π-orbitals in the reference configuration of EE, the degeneracy of these orbitals is slightly lifted which results in loss of degeneracy of the ground ($^2\Pi$) level and the $^2\Delta$ (excited) level as observed in the case of all the EOM-EE methods. However, the EOM-SF methods retain the degeneracy

Table 3 Total energies of the ground state (Hartree) and vertical excitation energies (eV) of several low-lying excited states of CH radical calculated using the active space SF-EOM-CCSDT methods with ROHF and UHF references. Calculations performed at the experimental ground state geometry *r*(CH) = 1.1198 Å, using the cc-pVTZ basis set with one frozen core orbital

Method	$\tilde{X}^2\Pi$	$\tilde{X}'^2\Pi$[a]	$a^4\Sigma^-$	$A^2\Delta$[b]	$A^2\Delta$[c]	$B^2\Sigma^-$	$C^2\Sigma^+$
UHF-EE-EOM-CCSD	−38.407096	0.015	1.204	3.210	3.223	4.590	5.521
UHF-EE-EOM-CC(2,3)	−38.411018	0.017	0.743	3.009	3.004	3.343	4.113
UHF-EE-EOM-CCSDT	−38.411021	0.0022	0.725	2.995	2.991	3.334	4.103
UHF-EE-EOM-CCSDT(SP)	−38.411022	0.0022	0.725	2.995	2.992	3.334	4.103
ROHF-EE-EOM-CCSD	−38.406975	0.007	0.991	3.205	3.295	4.402	5.402
ROHF-EE-EOM-CC(2,3)	−38.410986	0.016	0.738	3.000	2.998	3.340	4.117
ROHF-EE-EOM-CCSDT	−38.410988	0.0002	0.719	2.986	2.984	3.329	4.097
ROHF-EE-EOM-CCSDT(SP)	−38.410987	0.0002	0.719	2.986	2.984	3.329	4.097
UHF-SF-EOM-CCSD	−38.407473	0.0	0.687	2.991	2.991	3.343	4.118
UHF-SF-EOM-CC(2,3)	−38.410184	0.0	0.709	2.965	2.965	3.332	4.056
UHF-SF-EOM-CCSDT	−38.410934	0.0	0.703	2.962	2.962	3.325	4.061
UHF-SF-EOM-CCSDT(SP)	−38.410934	0.0	0.703	2.962	2.962	3.325	4.061
ROHF-SF-EOM-CCSD	−38.407607	0.0	0.687	2.985	2.985	3.350	4.110
ROHF-SF-EOM-CC(2,3)	−38.410211	0.0	0.707	2.963	2.963	3.324	4.054
ROHF-SF-EOM-CCSDT	−38.410974	0.0	0.702	2.960	2.960	3.317	4.059
ROHF-SF-EOM-CCSDT(SP)	−38.410973	0.0	0.702	2.960	2.960	3.317	4.059
Experiment (vertical)[d]			0.745	2.880		3.263	3.943

[a] The $X'^2\Pi$ state is the EOM target state in both EE and SF. The $X^2\Pi$ is the reference in EE, whereas a target state in SF. [b] The open-shell component of the $A^2\Delta$ state. [c] The closed-shell component of the $^2\Delta$ state. [d] Estimated from adiabatic excitation energies within the harmonic approximation for the excited state PES using experimental data (ref. 83).

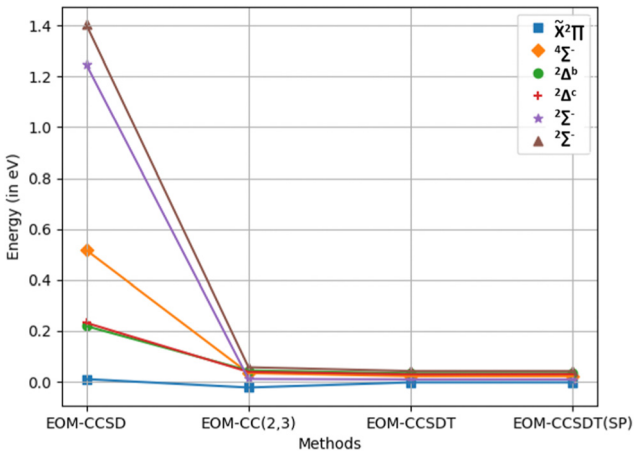

Fig. 3 Truncation error ($\Delta E_{EE} - \Delta E_{SF}$) for various truncation levels of EOM-CC.

due to the uniform distribution of electrons between the degenerate frontier MOs in the high-spin reference configuration. Secondly, the total energies and the excitation energies computed by the EE and SF variants for the same set of electronic states differ significantly, with a systematic overestimation of the EE computed values, compared to the SF values.

This discrepancy, in a sense, can be considered as a truncation error as it is expected to vanish in the FCI limit. As we move from EOM-CCSD to EOM-CCSDT *via* EOM-CC(2,3), the truncation error indeed decreases gradually for all the states. The trends in the truncation error in the UHF-based energies and excitation energies are summarized in Fig. 3.

The trends for ROHF-based ones are very similar. The maximum truncation errors are 1.403 eV for EOM-CCSD, 0.057 eV for EOM-CC(2,3), 0.042 eV for EOM-CCSDT with DP and 0.042 eV for EOM-CCSDT with SP when the UHF reference is used. If the ROHF reference is employed, the maximum truncation errors are 1.292 eV for EOM-CCSD, 0.063 eV for EOM-CC(2,3), 0.038 eV for EOM-CCSDT with DP and 0.038 eV for EOM-CCSDT with SP.

As we move from EOM-CCSD to EOM-CCSDT, the computed excitation energy values come closer to the experimental values in general, with an exception for the $^4\Sigma^-$ state, for which the EOM-CC(2,3) values are rather closer to the experimental values than are the EOM-CCSDT values.

3.4 Bond dissociation of the HF molecule

At equilibrium and near-equilibrium geometries, the ground state of the HF molecule is fairly non-degenerate, dominated by the electronic configuration, [core],$1\sigma^2 1\sigma^{*2} 1\pi^2 2\pi^2$ as the LUMO 2σ is well separated in energy from the HOMO. At these geometries, the ground state properties can be accurately computed using CCSD or CCSDT. However, upon bond-stretching, the HOMO–LUMO gap keeps on reducing and the ground state gains multi-reference character in the bond dissociation limit. The strong static correlation demands the use of SF-EOM-CCSDT for correctly targeting the ground state, starting with a high-spin triplet reference.

Table 4 presents the FCI/6-31G total energies of the HF ground state and the errors in the energies (δE) relative to FCI for various SF-EOM models using both the ROHF and the UHF references. Fig. 4 summarises the trends. The maximum absolute errors (MAE)s in ROHF based SF-EOM-CC methods, namely, SDT, SDT(SP) and SD are, respectively, 0.014 eV, 0.014 eV and 0.212 eV. For UHF-based models also, the MAEs are very similar. The discrepancy between UHF and ROHF is very small (of the order of a few micro-Hartrees).

The non-parallelity error (NPE) is another parameter to test the accuracy of the method, which is the difference between the

Table 4 FCI/6-31G total (ground state) energies (Hartree) and relative errors (eV) for various SF-EOM-CC/6-31G methods using ROHF and UHF references

R_{HF} (in Angs)	E_{FCI}[a]	δE_{SDT}^{ROHF}	δE_{SDT}^{ROHF} (SP)	δE_{SDT}^{UHF}	δE_{SDT}^{UHF} (SP)	δE_{SD}^{ROHF}	δE_{SD}^{UHF}
0.7	−100.00548	0.00939	0.00937	0.00952	0.00950	−0.07093	−0.06898
0.8	−100.08713	0.01018	0.01016	0.01035	0.01032	−0.05944	−0.05809
0.9	−100.11425	0.01019	0.01015	0.01028	0.01024	−0.04567	−0.04490
0.95	−100.11669	0.01032	0.01027	0.01034	0.01029	−0.03876	−0.03816
1.0	−100.11462	0.01052	0.01048	0.01054	0.01049	−0.03165	−0.03112
1.1	−100.10211	0.01129	0.01128	0.01129	0.01126	−0.01495	−0.01445
1.2	−100.08393	0.01240	0.01239	0.01237	0.01239	0.00725	0.00761
1.2764	−100.06870	0.01282	0.01282	0.01278	0.01277	0.02845	0.02855
1.4	−100.04428	0.01374	0.01375	0.01374	0.01376	0.06917	0.06867
1.6	−100.00975	0.01385	0.01387	0.01400	0.01403	0.14132	0.14005
1.8	−99.984078	0.01250	0.01251	0.01270	0.01272	0.19832	0.19704
2.0	−99.967201	0.01034	0.01035	0.01058	0.01059	0.21256	0.21210
2.1	−99.961487	0.00931	0.00943	0.00955	0.00958	0.19984	0.19996
2.2	−99.957183	0.00841	0.00849	0.00865	0.00868	0.17737	0.17802
2.4	−99.951656	0.00703	0.00705	0.00724	0.00723	0.12359	0.12481
2.6	−99.948741	0.00629	0.00630	0.00643	0.00641	0.08077	0.08214
2.8	−99.947238	0.00571	0.00570	0.00583	0.00581	0.05455	0.05594
3.0	−99.946465	0.00526	0.00525	0.00536	0.00535	0.04008	0.04153
3.2	−99.946065	0.00474	0.00473	0.00484	0.00482	0.03272	0.03417
3.4	−99.945857	0.00414	0.00413	0.00423	0.00420	0.02908	0.03051

[a] The FCI energies are taken from the ref. 84 and 85.

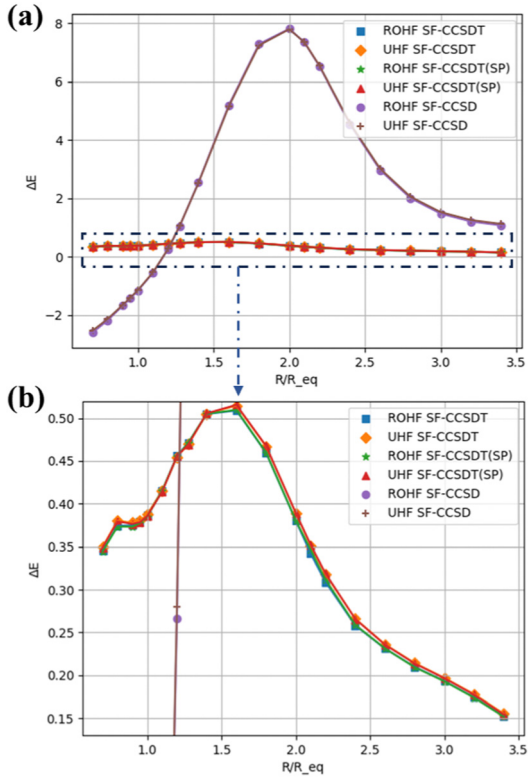

Fig. 4 Errors (δE, in millihartrees) relative to FCI in the ground-state total energies of the HF molecule using UHF and ROHF references. (a) Full range and (b) magnified range of SF-CCSDT.

maximum and minimum relative errors. For ROHF-based and UHF-based SF-EOM-CCSD, the NPEs are as high as 0.205 eV and 0.197 eV. For EOM-CCSDT (for DP as well as SP algorithms), the NPE reduces to 0.010 eV for both ROHF and UHF based variants.

4 Conclusions

In this article, we have presented our implementation of the SF-EOM-CCSDT method within Q-CHEM and its applications to study adiabatic energy gaps in CH_2 and NH_2^+ diradicals, vertical excitation energies of CH radicals and bond dissociation in the HF molecule. In CH_2 and NH_2^+ diradicals, the absolute errors in the energy gaps relative to the benchmarks are 0.01 eV or less. In bond dissociation of HF, the MAE and NPE for SF-EOM-CCSDT are, respectively, 0.014 eV and 0.010 eV. The difference between the EE and SF computed energy gaps between the same set of states is 0.001 eV or less at the EOM-CCSDT level as compared to 0.04 eV at the EOM-CCSD level as observed in the vertical excitation energies of CH. Using SP seldom introduces any significant error compared to DP. Rather, SP gives equally good results with a reduced computational cost (storage as well as RAM reduced by almost 50%), which not only leads to speed-up in the computations, but also widens the applicability of SF-EOM-CCSDT (and also EE-EOM-CCSDT) to bigger molecules for which the conventional DP algorithm may be computationally challenging.

Author contributions

Manisha contributed to software, validation and formal analysis. P. U. Manohar contributed to writing – review and editing, and supervision.

Data availability

The data supporting this article have been included as part of the ESI.†

Conflicts of interest

There are no conflicts to declare.

Appendix

The programmable expressions of SF-EOM-CCSDT within the Davidson's iterative diagonalization algorithm are presented below:

$$\sigma_i^a = ([\bar{H}_{SS} - E_{CC}]R_1)_i^a + (\bar{H}_{SD}R_2)_i^a + (\bar{H}_{ST}R_3)_i^a \quad (19)$$

$$\sigma_{ij}^{ab} = (\bar{H}_{DS}R_1)_{ij}^{ab} + ([\bar{H}_{DD} - E_{CC}]R_2)_{ij}^{ab} + (\bar{H}_{DT}R_3)_{ij}^{ab} \quad (20)$$

$$\sigma_{ijk}^{abc} = (\bar{H}_{TS}R_1)_{ijk}^{abc} + (\bar{H}_{TD}R_2)_{ijk}^{abc} + ([\bar{H}_{TT} - E_{CC}]R_3)_{ijk}^{abc} \quad (21)$$

The programmable expressions for SF-EOM/EE-EOM-CCSD were published by Levchenko *et al.*[16] Let these be referred to as "EOMCCSD-terms." The additional terms in EOM-CCSDT are given below:

$$(\bar{H}_{DS}R_1)_{ij}^{ab} = \text{EOMCCSD-terms} + \sum_{kc} F_{kc}^r t_{kij}^{cab}$$

$$(\bar{H}_{ST}R_3)_i^a = \langle \Phi_i^a | \bar{H} | R_3 \Phi_0 \rangle = 1/4 \sum_{jkbc} \langle jk \parallel bc \rangle r_{jki}^{bca}$$

$$(\bar{H}_{DT}R_3)_{ij}^{ab} = \left\langle \Phi_{ij}^{ab} | \bar{H} | R_3 \Phi_0 \right\rangle = \sum_{kc} F_{kc} r_{kij}^{cab} - P(ab) \sum_k I_{ijkb}^{2r_3} t_k^a - P(ij) \sum_c I_{j|c|a|b}^{3r_3} t_i^c + 1/2P(ij) \sum_{klc} \langle kl||ic \rangle r_{klj}^{cab} + 1/2P(ab) \sum_{kcd} \langle ka||cd \rangle r_{kij}^{cdb}$$

Table 5 Additional intermediates used in SF-EOM-CCSDT other than ref. 16

$$F^r_{ij} = \sum_a r^a_i f_{ja} + \sum_{ka} r^a_k \langle jk||ia\rangle + \sum_{kab} \left(r^a_i t^b_k \langle jk||ab\rangle + t^a_i r^b_k \langle jk||ab\rangle \right) + 1/2 \sum_{kbc} r^{bc}_{ik} \langle jk||bc\rangle$$

$$F^r_{ab} = -\sum_i r^a_i f_{ib} - \sum_{ic} r^c_i \langle ia||bc\rangle + \sum_{ijc} \left(r^c_i t^a_j \langle ij||bc\rangle + t^c_i r^a_j \langle ij||bc\rangle \right) - 1/2 \sum_{jkc} r^{ac}_{jk} \langle jk||bc\rangle$$

$$F^r_{ia} = \sum_{jb} \langle jk||ib\rangle r^b_j$$

$$I^{1r}_{iajb} = -\sum_k t^b_k \langle jk \parallel ia\rangle - \sum_c t^c_i \langle jb||ac\rangle + \sum_{kc} \left(r^c_i t^b_k \langle jk||ac\rangle + r^c_i t^b_k \langle jk||ac\rangle \right) - \sum_{kc} r^{bc}_{ik} \langle jk||ac\rangle$$

$$I^{4r}_{ijkl} = P(ij) \sum_a \langle kl||ia\rangle r^a_j + 1/2 \sum_{ab} tt^r_{ijab} \langle kl||ab\rangle$$

$$I^{5r}_{abcd} = -P(ab) \sum_i r^a_i \langle ib||cd\rangle + 1/2 \sum_{ij} tt^r_{ijab} \langle ij||cd\rangle$$

$$I^{2r}_{ijka} = -\sum_l I^4_{ijkl} r^a_l - \sum_l I^{4r}_{ijkl} t^a_l + 1/2 \sum_{cd} \langle ka||cd\rangle tt^r_{ijcd} + P(ij) \sum_{blc} \langle kl||bc\rangle r^{ac}_{jl} t^b_i + P(ij) \sum_{blc} \langle kl||bc\rangle t^{ac}_{jl} r^b_i - P(ij) \sum_b \langle ka \parallel jb\rangle r^b_i - P(ij) \sum_{lc} \langle kl||jc\rangle r^{ac}_{il}$$
$$+ \sum_{blc} \langle kl||bc\rangle r^b_l t^{ac}_{ij} + 1/2 \sum_{blc} \langle lk||cb\rangle r^{abc}_{jil}$$

$$I^{3r}_{iabc} = -\sum_d I^5_{bcad} r^d_i - \sum_d I^{5r}_{bcad} t^d_i + 1/2 \sum_{jk} \langle jk||ia\rangle tt^r_{jkbc} + P(bc) \sum_j \langle jk||ia\rangle r^c_j - \sum jkd \langle jk||ad\rangle r^{bd}_{ik} t^c_j - \sum_{jkd} \langle jk||ad\rangle t^{bd}_{ik} r^c_j - \sum_{kd} \langle kc||ad\rangle r^{bd}_{ik}$$
$$- 1/2 \sum_{kjd} \langle kj||da\rangle r^{dcb}_{kji}$$

$$I^2_{ijka} = I^2_{ijka} - (\text{from ref. 16}) + 1/2 \sum_{blc} \langle lk||cb\rangle t^{abc}_{jil}$$

$$I^3_{iabc} = I^3_{iabc} - (\text{from ref. 16}) - 1/2 \sum_{kjd} \langle kj||da\rangle t^{dcb}_{kji}$$

$$tt^r_{ijab} = r^{ab}_{ij} + P(ab)P(ij) t^a_i r^b_j$$

$$I^{2r_3}_{ijka} = 1/2 \sum_{lbc} \langle lk||bc\rangle r^{acb}_{jil}$$

$$I^{3r_3}_{iabc} = -1/2 \sum_{jkd} \langle jk||ad\rangle r^{bcd}_{ijk}$$

For computational convenience, we express the σ^{abc}_{ijk} as follows:

$$\sigma^{abc}_{ijk} = \left\langle \Phi^{abc}_{ijk} | \bar{H} | R_1 \Phi_0 \right\rangle + \left\langle \Phi^{abc}_{ijk} | \bar{H} | R_2 \Phi_0 \right\rangle + \left\langle \Phi^{abc}_{ijk} | \bar{H} | R_3 \Phi_0 \right\rangle$$
$$= P(ij|k) \left[-\sum_l F_{kl} r^{abc}_{ijl} + \sum_{lm} I^4_{ijlm} r^{abc}_{lmk} \right]$$
$$+ P(ab|c) \left[\sum_d F_{cd} r^{abd}_{ijk} + \sum_{de} I^5_{abde} r^{dec}_{ljk} \right]$$
$$+ P(ij|k) P(a|bc) \times \left[\sum_i I^{2r}_{ijla} t^{bc}_{kl} + \sum_d I^{3r}_{kdbc} t^{ad}_{lj} \right]$$
$$- P(a|bc) P(i|jk) \sum_{dl} I^1_{idla} r^{dbc}_{ljk}$$
$$+ P(ij|k) P(a|bc) \times \left[\sum_i I^2_{ijla} r^{bc}_{kl} - \sum_d I^3_{kdbc} r^{ad}_{lj} \right]$$
$$+ P(ij|k) \left[-\sum_l F^r_{kl} t^{abc}_{ijl} + \sum_{lm} I^{4r}_{ijlm} t^{abc}_{lmk} \right]$$
$$+ P(ab|c) \left[\sum_d F^r_{cd} t^{abd}_{ijk} + \sum_{de} I^{5r}_{abde} t^{dec}_{ljk} \right]$$

The intermediates used in the above expressions are mostly used from the EOM-CCSD intermediates given in ref. 16. The additional intermediates used in these expressions are summarized in Table 5.

Acknowledgements

Manisha is thankful to BITS Pilani for the institute fellowship.

Notes and references

1 T. Helgaker, P. Jorgensen and J. Olsen, *Molecular electronic-structure theory*, John Wiley & Sons, 2013.
2 J. Čížek, *J. Chem. Phys.*, 1966, **45**, 4256–4266.
3 D. Rowe, *Rev. Mod. Phys.*, 1968, **40**, 153.
4 O. Sĭnanoğlu and K. A. Brueckner, *Three approaches to electron correlation in atoms*, 1970.
5 H. Sekino and R. J. Bartlett, *Int. J. Quantum Chem.*, 1984, **26**, 255–265.
6 H. Koch, H. J. Jensen, T. Helgaker, G. E. Scuseria and H. F. Schaefer, *et al.*, *J. Chem. Phys.*, 1990, **92**, 4924–4940.
7 J. F. Stanton and R. J. Bartlett, *J. Chem. Phys.*, 1993, **98**, 7029–7039.
8 H. G. Kümmel, *Int. J. Mod. Phys. B*, 2003, **17**, 5311–5325.
9 R. J. Bartlett and M. Musiał, *Rev. Mod. Phys.*, 2007, **79**, 291.
10 P. U. Manohar and S. Pal, *Chem. Phys. Lett.*, 2007, **438**, 321–325.
11 P. U. Manohar, K. R. Shamasundar, A. Bag, N. Vaval and S. Pal, *Recent Progress in Coupled Cluster Methods: Theory and Applications*, 2010, pp. 375–393.
12 J. F. Stanton and J. Gauss, *J. Chem. Phys.*, 1994, **101**, 8938–8944.
13 M. Nooijen and R. J. Bartlett, *J. Chem. Phys.*, 1997, **107**, 6812–6830.

14 K. Kowalski and P. Piecuch, *J. Chem. Phys.*, 2000, **113**, 8490–8502.
15 L. V. Slipchenko and A. I. Krylov, *J. Chem. Phys.*, 2002, **117**, 4694–4708.
16 S. V. Levchenko and A. I. Krylov, *J. Chem. Phys.*, 2004, **120**, 175–185.
17 P. U. Manohar, L. Koziol and A. I. Krylov, *J. Phys. Chem. A*, 2009, **113**, 2591–2599.
18 A. Ünal and U. Bozkaya, *J. Chem. Theory Comput.*, 2022, **18**, 1489–1500.
19 R. J. Bartlett, *Geometrical Derivatives of Energy Surfaces and Molecular Properties*, Springer, 1986, pp. 35–61.
20 H. J. Monkhorst, *Int. J. Quantum Chem.*, 1977, **12**, 421–432.
21 A. I. Krylov, *Annu. Rev. Phys. Chem.*, 2008, **59**, 433–462.
22 D. Mukherjee, R. K. Moitra and A. Mukhopadhyay, *Mol. Phys.*, 1977, **33**, 955–969.
23 I. Lindgren, *Int. J. Quantum Chem.*, 1978, **14**, 33–58.
24 S. Pal, M. Rittby, R. J. Bartlett, D. Sinha and D. Mukherjee, *Chem. Phys. Lett.*, 1987, **137**, 273–278.
25 S. Pal, M. Rittby, R. J. Bartlett, D. Sinha and D. Mukherjee, *J. Chem. Phys.*, 1988, **88**, 4357–4366.
26 B. Jeziorski and H. J. Monkhorst, *Phys. Rev. A: At., Mol., Opt. Phys.*, 1981, **24**, 1668.
27 I. Lindgren and D. Mukherjee, *Phys. Rep.*, 1987, **151**, 93–127.
28 J. Malrieu, P. Durand and J. Daudey, *J. Phys. A: Math. Gen.*, 1985, **18**, 809.
29 D. Mukherjee and S. Pal, *Adv. Quantum Chem.*, 1989, **20**, 291–373.
30 D. Kumar and P. U. Manohar, *Chem. Phys. Lett.*, 2019, **730**, 234–238.
31 M. Head-Gordon, T. Lee and R. Bartlett, *Modern Ideas in Coupled Cluster Theory*, 1997.
32 H. Koch, H. J. Jensen and T. Helgaker, *et al.*, *J. Chem. Phys.*, 1990, **93**, 3345–3350.
33 H. Sekino and R. J. Bartlett, *Int. J. Quantum Chem.*, 1984, **26**, 255–265.
34 H. Nakatsuji and K. Hirao, *J. Chem. Phys.*, 1978, **68**, 2053–2065.
35 H. Nakatsuji, *Chem. Phys. Lett.*, 1991, **177**, 331–337.
36 M. Nooijen and R. J. Bartlett, *J. Chem. Phys.*, 1997, **106**, 6441–6448.
37 M. Nooijen, K. Shamasundar and D. Mukherjee, *Mol. Phys.*, 2005, **103**, 2277–2298.
38 H. Bethe, *Z. Phys.*, 1931, **71**, 205–226.
39 T.-I. Shibuya and V. McKoy, *Phys. Rev. A: At., Mol., Opt. Phys.*, 1970, **2**, 2208–2218.
40 A. V. Luzanov, *Theor. Exp. Chem.*, 1982, **17**, 227–234.
41 A. I. Krylov, *Chem. Phys. Lett.*, 2001, **338**, 375–384.
42 S. Hirata, M. Nooijen and R. J. Bartlett, *Chem. Phys. Lett.*, 2000, **326**, 255–262.
43 K. Hald, P. Jørgensen, J. Olsen and M. Jaszuński, *J. Chem. Phys.*, 2001, **115**, 671–679.
44 H. Larsen, K. Hald, J. Olsen and P. Jørgensen, *J. Chem. Phys.*, 2001, **115**, 3015–3020.
45 D. Casanova, L. V. Slipchenko, A. I. Krylov and M. Head-Gordon, *J. Chem. Phys.*, 2009, **130**, 044103.
46 D. Casanova, *J. Chem. Phys.*, 2012, **137**, 084105.
47 L. V. Slipchenko and A. I. Krylov, *J. Chem. Phys.*, 2003, **118**, 6874–6883.
48 T. Wang and A. I. Krylov, *J. Chem. Phys.*, 2005, **123**, 104304.
49 N. Orms and A. I. Krylov, *Phys. Chem. Chem. Phys.*, 2018, **20**, 13127–13144.
50 Y. Shao, M. Head-Gordon and A. I. Krylov, *J. Chem. Phys.*, 2003, **118**, 4807–4818.
51 A. I. Krylov and C. D. Sherrill, *J. Chem. Phys.*, 2002, **116**, 3194–3203.
52 A. I. Krylov, *Acc. Chem. Res.*, 2006, **39**, 83–91.
53 P. Pokhilko, D. Izmodenov and A. I. Krylov, *J. Chem. Phys.*, 2020, **152**, 034105.
54 T. Wang and A. I. Krylov, *Chem. Phys. Lett.*, 2006, **425**, 196–200.
55 A. I. Krylov, *J. Phys. Chem. A*, 2005, **109**, 10638–10645.
56 L. Koziol, M. Winkler, Houk, S. Venkataramani, W. Sander and A. I. Krylov, *J. Phys. Chem. A*, 2007, **111**, 5071–5080.
57 L. V. Slipchenko and A. I. Krylov, *J. Chem. Phys.*, 2003, **118**, 9614–9622.
58 S. Gibson, J. Greene and J. Berkowitz, *J. Chem. Phys.*, 1985, **83**, 4319–4328.
59 S. A. Kucharski, M. Włoch, M. Musiał and R. J. Bartlett, *J. Chem. Phys.*, 2001, **115**, 8263–8266.
60 J. D. Watts and R. J. Bartlett, *J. Chem. Phys.*, 1994, **101**, 3073–3078.
61 J. D. Watts and R. J. Bartlett, *Chem. Phys. Lett.*, 1995, **233**, 81–87.
62 J. D. Watts and R. J. Bartlett, *Chem. Phys. Lett.*, 1996, **258**, 581–588.
63 H. Koch, O. Christiansen, P. Jørgensen and J. Olsen, *Chem. Phys. Lett.*, 1995, **244**, 75–82.
64 O. Christiansen, H. Koch and P. Jørgensen, *J. Chem. Phys.*, 1995, **103**, 7429–7441.
65 O. Christiansen, H. Koch and P. Jørgensen, *J. Chem. Phys.*, 1996, **105**, 1451–1459.
66 K. Kowalski and P. Piecuch, *J. Chem. Phys.*, 2001, **115**, 643–651.
67 M. Kállay and P. R. Surján, *J. Chem. Phys.*, 2000, **113**, 1359–1365.
68 P. U. Manohar and A. I. Krylov, *J. Chem. Phys.*, 2008, **129**, 194105.
69 K. Kowalski, *J. Chem. Phys.*, 2005, **123**, 014109.
70 L. Ravichandran, N. Vaval and S. Pal, *J. Chem. Theory Comput.*, 2011, **7**, 876–883.
71 E. Epifanovsky, D. Zuev, X. Feng, K. Khistyaev, Y. Shao and A. I. Krylov, *J. Chem. Phys.*, 2013, **139**, 134105.
72 Y. Shao, Z. Gan, E. Epifanovsky, A. T. Gilbert, M. Wormit, J. Kussmann, A. W. Lange, A. Behn, J. Deng and X. Feng, *et al.*, *Mol. Phys.*, 2015, **113**, 184–215.
73 S. A. Kucharski, M. Włoch, M. Musiał and R. J. Bartlett, *J. Chem. Phys.*, 2001, **115**, 8263–8266.
74 P. Pokhilko, E. Epifanovsky and A. I. Krylov, *J. Chem. Theory Comput.*, 2018, **14**, 4088–4096.
75 *ANSI/IEEE Std 754-1985*, 1985, pp. 1–20.
76 A. I. Krylov, C. D. Sherrill and M. Head-Gordon, *J. Chem. Phys.*, 2000, **113**, 6509–6527.

77 C. Davidson, *J. Comput. Phys.*, 1975, **17**, 87–94.
78 K. Hirao and H. Nakatsuji, *J. Comput. Phys.*, 1982, **45**, 246–254.
79 E. Epifanovsky, A. T. Gilbert, X. Feng, J. Lee, Y. Mao, N. Mardirossian, P. Pokhilko, A. F. White, M. P. Coons and A. L. Dempwolff, *et al.*, *J. Chem. Phys.*, 2021, **155**, 084801.
80 C. D. Sherrill, M. L. Leininger, T. J. Van Huis and H. F. Schaefer III, *J. Chem. Phys.*, 1998, **108**, 1040–1049.
81 J. C. Stephens, Y. Yamaguchi, C. D. Sherrill and H. F. Schaefer, *J. Phys. Chem. A*, 1998, **102**, 3999–4006.
82 L. V. Slipchenko and A. I. Krylov, *J. Chem. Phys.*, 2005, **123**, 084107.
83 G. Herzberg, *Mol. Spectra Mol. Struct.*, 1950, **1**, 127.
84 A. I. Krylov, *Chem. Phys. Lett.*, 2001, **338**, 375–384.
85 J. S. Sears, C. D. Sherrill and A. I. Krylov, *J. Chem. Phys.*, 2003, **118**, 9084–9094.

